X-ray scattering studies of 7O.7 demonstrated that the smectic-F phase set in for a narrow temperature range in films as thick as 180 layers, and that the temperature range increases with decreasing layer number. For films of the order of 25 layers thick, the smectic-I phase is observed at approximately 334 K, and with decreasing thickness the temperature range for this phase also increases. Below approximately 10 to 15 layers, the smectic-I phase extends up to $\sim$ 342 K where bulk samples undergo a first-order transition from the crystalline-B to the smectic-C phase. Synchrotron X-ray scattering experiments show that, in thin films (five layers for example), the homogeneous smectic-I film undergoes a first-order transition to one in which the two surface layers are smectic-I and the three interior layers are smectic-C (Sirota *et al.*, 1985; Sirota, Pershan, Sorensen & Collett, 1987). The fact that two phases with the same symmetry can coexist in this manner tells us that in this material there is some important microscopic difference between them. This is reaffirmed by the fact that the phase transition from the surface smectic-I to the homogeneous smectic-C phase has been observed to be first order (Sorensen *et al.*, 1987).

In contrast to 7O.7, Birgeneau and co-workers found that in racemic 4-(2-methylbutyl)phenyl 4′-octyloxylbiphenyl-4-carboxylate (8OSI) (Brock *et al.*, 1986), the X-ray structure of the smectic-I phase evolves continuously into that of the smectic-C. By applying a magnetic field to a thick freely suspended sample, Brock *et al.* were able to obtain a large monodomain sample. They measured the X-ray scattering intensity around the circle in the reciprocal-space plane shown in Fig. 4.4.4.4(*b*) that passes through the peaks. For higher temperatures, when the sample is in the smectic-C phase, the intensity is essentially constant around the circle; however, on cooling, it gradually condenses into six peaks, separated by 60°. The data were analysed by expressing the intensity as a Fourier series of the form

$$S(\chi) = I_0\left[\tfrac{1}{2} + \sum_{n=1}^{\infty} C_{6n}\cos 6n(90^\circ - \chi)\right] + I_B,$$

where I_0 fixes the absolute intensity and I_B fixes the background. The temperature variation of the coefficients scaled according to the relation $C_{6n} = C_6^{\sigma n}$ where the empirical relation $\sigma_n = 2.6(n-1)$ is in good agreement with a theoretical form predicted by Aharony *et al.* (1986). The only other system in which this type of measurement has been made was the smectic-C phase of 7O.7 (Collett, 1983). In that case, the intensity around the circle was constant, indicating the absence of any tilt-induced bond orientational order (Aharony *et al.*, 1986).

It would appear that the near-neighbour molecular packing of the smectic-I and the crystalline-J phases is the same, in just the same way as for the packing of the smectic-F and the crystalline-G phases. The four smectic-I widths analogous to those illustrated in Fig. 4.4.4.4(*a*) are, like that of the smectic-F, both anisotropic and temperature dependent (Sirota *et al.*, 1985; Sirota, Pershan, Sorensen & Collett, 1987; Brock *et al.*, 1986; Benattar *et al.*, 1979).

4.4.4.3. *Crystalline phases with molecular rotation*

4.4.4.3.1. *Crystal-B*

Recognition of the distinction between the hexatic-B and crystalline-B phases provided one of the more important keys to understanding the ordered mesomorphic phases. There are a number of distinct phases called crystalline-B that are all true three-dimensional crystals, with resolution-limited Bragg peaks (Moncton & Pindak, 1979; Aeppli *et al.*, 1981). The feature common to them all is that the average molecular orientation is normal to the layers, and within each layer the molecules are distributed on a triangular lattice. In view of the 'blade-like' shape of the molecule, the hexagonal site symmetry implies that the molecules must be rotating rapidly (Levelut & Lambert, 1971; Levelut, 1976; Richardson *et al.*, 1978). We have previously remarked that this apparent rotational motion characterizes all of the phases listed in Table 4.4.1.1 except for the crystalline-E, -H and -K. In the most common crystalline-B phase, adjacent layers have *ABAB*-type stacking (Leadbetter, Gaughan *et al.*, 1979; Leadbetter, Mazid & Kelly, 1979). High-resolution studies on well oriented samples show that in addition to the Bragg peaks the crystalline-B phases have rods of relatively intense diffuse scattering distributed along the 10*L* Bragg peaks (Moncton & Pindak, 1979; Aeppli *et al.*, 1981). The widths of these rods in the reciprocal-space direction, parallel to the layers, are very sharp, and without a high-resolution spectrometer their widths would appear to be resolution limited. In contrast, along the reciprocal-space direction normal to the layers, their structure corresponds to the molecular form factor.

If the intensity of the diffuse scattering can be represented as proportional to $\langle \mathbf{Q}\cdot\mathbf{u}\rangle^2$, where $\mathbf{u}$ describes the molecular displacement, the fact that there is no rod of diffuse scattering through the 00*L* peaks indicates that the rods through the 10*L* peaks originate from random disorder in 'sliding' displacements of adjacent layers. It is likely that these displacements are thermally excited phonon vibrations; however, we cannot rule out some sort of non-thermal static defect structure. In any event, assuming this diffuse scattering originates in a thermal vibration for which adjacent layers slide over one another with some amplitude $\langle \mathbf{u}^2\rangle^{1/2}$, and assuming strong coupling between this shearing motion and the molecular tilt, we can define an angle $\varphi = \tan^{-1}(\langle \mathbf{u}^2\rangle^{1/2}/d)$, where d is the layer thickness. The observed diffuse intensity corresponds to angles φ between 3 and 6° (Aeppli *et al.*, 1981).

Leadbetter and co-workers demonstrated that in the *n*O.*m* series various molecules undergo a series of restacking transitions and that crystalline-B phases exist with *ABC* and *AAA* stacking as well as the more common *ABAB* (Leadbetter, Mazid & Richardson 1980; Leadbetter, Mazid & Kelly, 1979). Subsequent high-resolution studies on thick freely suspended films revealed that the restacking transitions were actually subtler, and in 7O.7, for example, on cooling the hexagonal *ABAB* phase one observes an orthorhombic and then a monoclinic phase before the hexagonal *AAA* (Collett *et al.*, 1982, 1985). Furthermore, the first transition from the hexagonal *ABAB* to the monoclinic phase is accompanied by the appearance of a relatively long wavelength modulation within the plane of the layers. The polarization of this modulation is along the layer normal, or orthogonal to the polarization of the displacements that gave rise to the rods of thermal diffuse scattering (Gane & Leadbetter, 1983).

It is also interesting to note that the *AAA* simple hexagonal structure does not seem to have been observed outside liquid-crystalline materials and, were it not for the fact that the crystalline-B hexagonal *AAA* is always accompanied by long wavelength modulations, it would be the only case of which we are aware.

Figs. 4.4.4.6(*a*) and (*b*) illustrate the reciprocal-space positions of the Bragg peaks (dark dots) and modulation-induced side bands (open circles) for the unmodulated hexagonal *ABAB* and the modulated orthorhombic phase (Collett *et al.*, 1984). For convenience, we only display one 60° sector. Hirth *et al.* (1984) explained how both the reciprocal-space structure and the modulation of the orthorhombic phase could result from an ordered array of partial dislocations. They were not, however, able to provide a specific model for the microscopic driving force for the transition. Sirota, Pershan & Deutsch (1987) proposed a variation of the Hirth model in which the dislocations pair up to form a wall of dislocation dipoles such that within the wall the local molecular packing is essentially identical to the packing in the crystalline-G phase that appears at temperatures just below the crystalline-B phase. This model explains: (1) the macroscopic symmetry of the

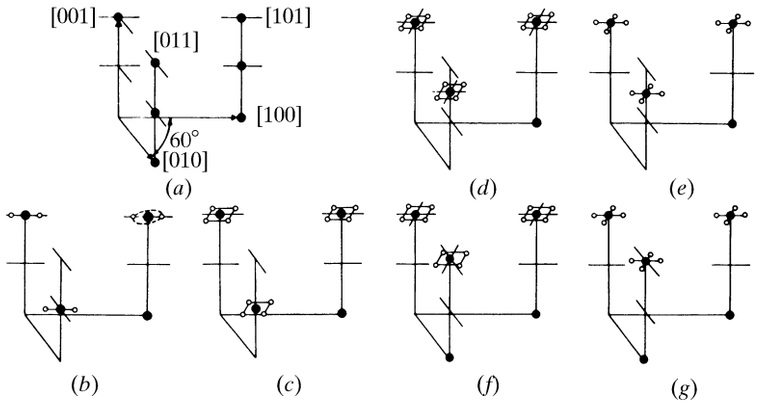

Fig. 4.4.4.6. Location of the Bragg peaks in one 60° section of reciprocal space for the three-dimensional crystalline-B phases observed in thick films of 7O.7. (*a*) The normal hexagonal crystalline-B phase with *ABAB* stacking. (*b*) The one-dimensional modulated phase with orthorhombic symmetry. The closed circles are the principal Bragg peaks and the open circles indicate side bands associated with the long-wavelength modulation. (*c*) The two-dimensional modulated phase with orthorhombic symmetry. Only the lowest-order side bands are shown. They are situated on the corners of squares surrounding the Bragg peak. The squares are oriented as shown and the amplitude of the square diagonal is equal to the distance between the two side bands illustrated in (*b*). (*d*) The two-dimensional modulated phase with monoclinic symmetry. Note that the L position of one of the peaks has shifted relative to (*c*). (*e*) A two-dimensional modulated phase with orthorhombic symmetry that is only observed on heating the quenched phase illustrated in (*g*). (*f*) The two-dimensional modulated phase with hexagonal symmetry and *AAA* layer stacking. (*g*) A two-dimensional hexagonal phase with *AAA* layer stacking that is only observed on rapid cooling from the phase shown in (*c*).

phase; (2) the period of the modulation; (3) the polarization of the modulation; and (4) the size of the observed deviations of the reciprocal-space structure from the hexagonal symmetry of the *ABAB* phase and suggests a microscopic driving mechanism that we will discuss below.

On further cooling, there is a first-order transition in which the one-dimensional modulation that appeared at the transition to orthorhombic symmetry is replaced by a two-dimensional modulation as shown in Fig. 4.4.4.6(*c*). On further cooling, there is another first-order transition in which the positions of the principal Bragg spots change from having orthorhombic to monoclinic symmetry as illustrated in Fig. 4.4.4.6(*d*). On further cooling, the Bragg peaks shift continually until there is one more first-order transition to a phase with hexagonal *AAA* positions as illustrated in Fig. 4.4.4.6(*f*). On further cooling, the *AAA* symmetry remains unchanged, and the modulation period is only slightly dependent on temperature, but the modulation amplitude increases dramatically. Eventually, as indicated in the phase diagram shown in Fig. 4.4.4.5, the system undergoes another first-order transition to the tilted crystalline-G phase. The patterns in Figs. 4.4.4.6(*e*) and (*g*) are observed by rapid quenching from the temperatures at which the patterns in Fig. 4.4.4.6(*b*) are observed.

Although there is not yet an established theoretical explanation for the origin of the 'restacking-modulation' effects, there are a number of experimental facts that we can summarize, and which indicate a probable direction for future research. Firstly, if one ignores the long wavelength modulation, the hexagonal *ABAB* phase is the only phase in the diagram for 7O.7 for which there are two molecules per unit cell. There must be some basic molecular effect that determines this particular coupling between every other layer. In addition, it is particularly interesting that it only manifests itself for a small temperature range and then vanishes as the sample is cooled. Secondly, any explanation for the driving force of the restacking transition must also explain the modulations that accompany it. In particular, unless one cools rapidly, the same modulation structures with the same amplitudes always appear at the same temperature, regardless of the sample history, *i.e.* whether heating or cooling. No significant hysteresis is observed and Sirota argued that the structures are in thermal equilibrium.

There are a number of physical systems for which the development of long-wavelength modulations is understood, and in each case they are the result of two or more competing interaction energies that cannot be simultaneously minimized (Blinc & Levanyuk, 1986; Safinya, Varady *et al.*, 1986; Lubensky & Ingersent, 1986; Winkor & Clarke, 1986; Moncton *et al.*, 1981; Fleming *et al.*, 1980; Villain, 1980; Frank & van der Merwe, 1949; Bak *et al.*, 1979; Pokrovsky & Talapov, 1979). The easiest to visualize is epitaxic growth of one crystalline phase on the surface of another when the two lattice vectors are slightly incommensurate. The first atomic row of adsorbate molecules can be positioned to minimize the attractive interactions with the substrate. This is slightly more difficult for the second row, since the distance that minimizes the interaction energy between the first and second rows of adsorbate molecules is not necessarily the same as the distance that would minimize the interaction energy between the first row and the substrate. As more and more rows are added, the energy price of this incommensurability builds up, and one possible configuration that minimizes the global energy is a modulated structure.

In all known cases, the very existence of modulated structures implies that there must be competing interactions, and the only real question about the modulated structures in the crystalline-B phases is the identification of the competing interactions. It appears that one of the more likely possibilities is the difficulty in packing the 7O.7 molecules within a triangular lattice while simultaneously optimizing the area per molecule of the alkane tails and the conjugated rings in the core (Carlson & Sethna, 1987; Sadoc & Charvolin, 1986). Typically, the mean cross-sectional area for a straight alkane in the all-*trans* configuration is between 18 and 19 $\mathring{A}^2$, while the mean area per molecule in the crystalline-B phase is closer to 24 $\mathring{A}^2$. While these two could be reconciled by assuming that the alkanes are tilted with respect to the conjugated core, there is no reason why the angle that reconciles the two should also be the same angle that minimizes the internal energy of the molecule. Even if it were the correct angle at some temperature by accident, the average area per chain is certainly temperature dependent. Even without attempting to include the rotational dynamics that are necessary to understanding the axial site symmetry, it is obvious that there can be a conflict in the packing requirements of the two different parts of the molecule.

A possible explanation of these various structures might be as follows: at high temperatures, both the alkane chain, as well as the

other degrees of freedom, have considerable thermal motions that make it possible for the conflicting packing requirements to be simultaneously reconciled by one or another compromise. On the other hand, with decreasing temperature, some of the thermal motions become frozen out, and the energy cost of the reconciliation that was possible at higher temperatures becomes too great. At this point, the system must find another solution, and the various modulated phases represent the different compromises. Finally, all of the compromises involving inhomogeneities, like the modulations or grain boundaries, become impossible and the system transforms into a homogeneous crystalline-G phase.

If this type of argument could be made more specific, it would also provide a possible explanation for the molecular origin of the three-dimensional hexatic phases. The original suggestion for the existence of hexatic phases in two dimensions was based on the fact that the interaction energy between dislocations in two dimensions was logarithmic, such that the entropy and the enthalpy had the same functional dependence on the density of dislocations. This gave rise to the observation that above a certain temperature two-dimensional crystals would be unstable against thermally generated dislocations. Although Litster and Birgeneau's suggestion that some of the observed smectic phases might be stacks of two-dimensional hexatics is certainly correct, it is not necessary that the observed three-dimensional hexatics originate from entropy-driven thermally excited dislocations. For example, the temperature–layer-number phase diagram for 7O.7 that is shown in Fig. 4.4.4.5 has the interesting property that the temperature region over which the tilted hexatic phases exist in thin films is almost the same as the temperature region for which the modulated phases exist in thick films and in bulk samples.

From the fact that molecules in the *n*O.*m* series that only differ by one or two —CH_2— groups have different sequences of mesomorphic phases, we learn that within any one molecule the difference in chemical potentials between the different mesomorphic phases must be very small (Leadbetter, Mazid & Kelly, 1979; Doucet & Levelut, 1977; Leadbetter, Frost & Mazid, 1979; Leadbetter, Mazid & Richardson, 1980; Smith *et al.*, 1973; Smith & Garland, 1973). For example, although in 7O.7 the smectic-F phase is only observed in finite-thickness films, both 5O.6 and 9O.4 have smectic-F phase in bulk. Thus, in bulk 7O.7 the chemical potential for the smectic-F phase must be only slightly larger than that of the modulated crystalline-B phases, and the effect of the surfaces must be sufficient to reverse the order in samples of finite thickness.

As far as the appearance of the smectic-F phase in 7O.7 is concerned, it is well known that the interaction energy between dislocation pairs is very different near a free surface from that in the bulk (Pershan, 1974; Pershan & Prost, 1975). The origin of this is that the elastic properties of the surface will usually cause the stress field of a dislocation near to the surface either to vanish or to be considerably smaller than it would in the bulk. Since the interaction energy between dislocations depends on this stress field, the surface significantly modifies the dislocation–dislocation interaction. This is a long-range effect, and it would not be surprising if the interactions that stabilized the dislocation arrays to produce the long-wavelength modulations in the thick samples were sufficiently weaker in the samples of finite thickness that the dislocation arrays are disordered. Alternatively, there is evidence that specific surface interactions favour a finite molecular tilt at temperatures where the bulk phases are uniaxial (Farber, 1985). Incommensurability between the period of the tilted surface molecules and the crystalline-B phases below the surface would increase the density of dislocations, and this would also modify the dislocation–dislocation interactions in the bulk.

Sirota *et al.* (1985) and Sirota, Pershan, Sorensen & Collett (1987) demonstrated that, while the correlation lengths of the smectic-F phase have a significant temperature dependence, the lengths are independent of film thickness, and this supports the argument that although the effects of the surface are important in stabilizing the smectic-F phase in 7O.7, once the phase is established it is essentially no different from the smectic-F phases observed in bulk samples of other materials. Brock *et al.* (1986) observed anisotropies in the correlation lengths of thick samples of 8OSI that are similar to those observed by Sirota.

These observations motivate the hypothesis that the dislocation densities in the smectic-F phases are determined by the same incommensurability that gives rise to the modulated crystalline-B structures. Although all of the experimental evidence supporting this hypothesis was obtained from the smectic-F tilted hexatic phase, there is no reason why this speculation could not apply to both the tilted smectic-I and the untilted hexatic-B phase.

4.4.4.3.2. *Crystal-G, crystal-J*

The crystalline-G and crystalline-J phases are the ordered versions of the smectic-F and smectic-I phases, respectively. The positions of the principal peaks illustrated in Fig. 4.4.4.4 for the smectic-F(I) are identical to the positions in the smectic-G(J) phase if small thermal shifts are discounted. In both the hexatic and the crystalline phases, the molecules are tilted with respect to the layer normals by approximately 25 to 30° with nearly hexagonal packing around the tilted axis (Doucet & Levelut, 1977; Levelut *et al.*, 1974; Levelut, 1976; Leadbetter, Mazid & Kelly, 1979; Sirota, Pershan, Sorensen & Collett, 1987). The interlayer molecular packing appears to be end to end, in an *AAA* type of stacking (Benattar *et al.*, 1983; Benattar *et al.*, 1981; Levelut, 1976; Gane *et al.*, 1983). There is only one molecule per unit cell and there is no evidence for the long-wavelength modulations that are so prevalent in the crystalline-B phase that is the next higher temperature phase above the crystalline-G in 7O.7.

4.4.4.4. *Crystalline phases with herringbone packing*

4.4.4.4.1. *Crystal-E*

Fig. 4.4.4.7 illustrates the intralayer molecular packing proposed for the crystalline-E phase (Levelut, 1976; Doucet, 1979; Levelut *et al.*, 1974; Doucet *et al.*, 1975; Leadbetter *et al.*, 1976; Richardson *et al.*, 1978; Leadbetter, Frost, Gaughan & Mazid, 1979; Leadbetter, Frost & Mazid, 1979). The molecules are, on average, normal to the

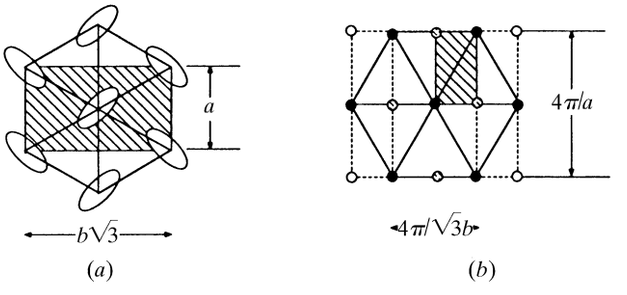

Fig. 4.4.4.7. (*a*) The 'herringbone' stacking suggested for the crystalline-E phase in which molecular rotation is partially restricted. The primitive rectangular unit cell containing two molecules is illustrated by the shaded region. The lattice has rectangular symmetry and $a \neq b$. (*b*) The position of the Bragg peaks in the plane in reciprocal space that is parallel to the layers. The dark circles indicate the principal Bragg peaks that would be the only ones present if all molecules were equivalent. The open circles indicate additional peaks that are observed for the model illustrated in (*a*). The cross-hatched circles indicate peaks that are missing because of the glide plane in (*a*).

references